



**HAL**  
open science

## **Functional characterization of a human POU1F1 mutation associated with isolated growth hormone deficiency: a novel etiology for IGHD**

Marie-Laure Sobrier, Yu-Cheng Tsai, Christelle Pérez, Bruno Leheup, Tahar Bouceba, Philippe Duquesnoy, Bruno Copin, Daria Sizova, Alfredo Penzo, Ben Z. Stanger, et al.

### ► To cite this version:

Marie-Laure Sobrier, Yu-Cheng Tsai, Christelle Pérez, Bruno Leheup, Tahar Bouceba, et al.. Functional characterization of a human POU1F1 mutation associated with isolated growth hormone deficiency: a novel etiology for IGHD. *Human Molecular Genetics*, 2016, 25 (3), pp.472-483. 10.1093/hmg/ddv486 . hal-01304122

**HAL Id: hal-01304122**

**<https://hal.sorbonne-universite.fr/hal-01304122>**

Submitted on 19 Apr 2016

**HAL** is a multi-disciplinary open access archive for the deposit and dissemination of scientific research documents, whether they are published or not. The documents may come from teaching and research institutions in France or abroad, or from public or private research centers.

L'archive ouverte pluridisciplinaire **HAL**, est destinée au dépôt et à la diffusion de documents scientifiques de niveau recherche, publiés ou non, émanant des établissements d'enseignement et de recherche français ou étrangers, des laboratoires publics ou privés.

1       **Functional characterization of a human *POU1F1* mutation associated with isolated growth**  
2                       **hormone deficiency (IGHD): a novel etiology for IGHD**

3

4 Marie-Laure Sobrier<sup>1\*</sup>, Yu-Cheng Tsai<sup>2</sup>, Christelle Pérez<sup>1</sup>, Bruno Leheup<sup>3</sup>, Tahar Bouceba<sup>4</sup>, Philippe  
5 Duquesnoy<sup>1</sup>, Bruno Copin<sup>5</sup>, Daria Sizova<sup>2</sup>, Alfredo Penzo<sup>6</sup>, Ben Z. Stanger<sup>6</sup>, Nancy E. Cooke<sup>2</sup>,  
6 Stephen A. Liebhaber<sup>2</sup>, and Serge Amselem<sup>1,5</sup>.

7       <sup>1</sup> Inserm UMRS933, Hôpital Trousseau, Sorbonne Universités, UPMC Univ Paris 06, Paris, France

8       <sup>2</sup> Department of Genetics, Perelman School of Medicine University of Pennsylvania, Philadelphia,  
9       USA

10       <sup>3</sup> Service de génétique clinique pédiatrique, Hôpital d'enfants, CHU Nancy, Vandoeuvre-Lès-Nancy,  
11       France

12       <sup>4</sup> Institut de Biologie Paris-Seine, Plateforme d'Interactions Moléculaires Fr 3631, UPMC, Paris,  
13       France

14       <sup>5</sup> Service de Génétique et d'Embryologie Médicales, Assistance Publique-Hôpitaux de Paris, Hôpital  
15       Armand Trousseau, Paris, France

16       <sup>6</sup> Gastroenterology Division, Department of Medicine, Perelman School of Medicine at the University  
17       of Pennsylvania, University of Pennsylvania, Philadelphia, USA.

18       Corresponding author:

19       Marie-Laure SOBRIER

20       UMRS933, Hôpital Trousseau, 26 avenue du Dr Netter, 75012 Paris, France

21       Phone: 33 1 44 73 52 42

22       Fax: 33 1 44 73 52 18

23       e-mail: marie-laure.sobrier@inserm.fr

24

25 **Abstract**

26 POU1F1, a pituitary-specific POU-homeo domain transcription factor, plays an essential role  
27 in specification of the somatotroph, lactotroph and thyrotroph lineages and in activation of *GHI*, *PRL*  
28 and *TSH $\beta$*  transcription. Individuals with mutations in *POU1F1* present with combined deficiency of  
29 GH, PRL, and TSH. Here we identified a heterozygous missense mutation with evidence of  
30 pathogenicity, at the *POU1F1* locus, in a large family in which isolated growth hormone deficiency  
31 segregates as an autosomal dominant trait. The corresponding p.Pro76Leu mutation maps to a  
32 conserved site within the POU1F1 transactivation domain. Bandshift assays revealed that the mutation  
33 alters wild-type POU1F1 binding to cognate sites within the *hGH-LCR* and *hGHI* promoter, but not to  
34 sites within the *PRL* promoter, and it selectively increases binding affinity to sites within the *hGH-*  
35 *LCR*. Co-immunoprecipitation studies reveal that this substitution enhances interactions of POU1F1  
36 with three of its cofactors, PITX1, LHX3a and ELK1, and that residue 76 plays a critical role in these  
37 interactions. Insertion of the mutation at the mouse *Pou1f1* locus results in a dramatic loss of protein  
38 expression despite normal mRNA concentrations. Mice heterozygous for the p.Pro76Leu mutation  
39 were phenotypically normal while homozygotes demonstrated a dwarf phenotype. Overall, this study  
40 unveils the involvement of *POU1F1* in dominantly inherited isolated GH deficiency and demonstrates  
41 a significant impact of the Pro76Leu mutation on DNA binding activities, alterations in transactivating  
42 functions and interactions with cofactors. Our data further highlight difficulties in modeling human  
43 genetic disorders in the mouse despite apparent conservation of gene expression pathways and  
44 physiologic functions.

## 45 **Introduction**

46 Pituitary development is temporally and spatially regulated by numerous signaling molecules  
47 and transcription factors (1). The Pou-homeodomain protein, Pou1f1, initially named Pit1, plays a key  
48 role in development of the anterior pituitary. Pou1f1 autoregulates its own expression (2, 3) and the  
49 expression of the three signature hormones [growth hormone (Gh), prolactin (Prl) and thyroid-  
50 stimulating hormone beta subunit (Tsh $\beta$ )]. As such, Pou1f1 serves essential functions in differentiation  
51 and proliferation of somatotropes, lactotropes and thyrotropes. The loss of POU1F1 functions results  
52 in combined pituitary hormone deficiency syndromes in both mice and humans.

53 The Pou1f1 protein (291 amino acids) is composed of an N-terminal transactivating domain  
54 (TAD) (4) involved in protein-protein interactions, and a homeodomain comprising Pou-specific and  
55 Pou-Homeo domains involved in DNA binding and in interactions with transcriptional cofactors (2).  
56 Pou1f1 recognizes a weakly conserved A/T-rich consensus sequence (A/T)(A/T)TATNCAT, binds to  
57 well-defined sites within the promoters and/or enhancers of multiple target genes (5, 6), and stimulates  
58 gene transcription in concert with a number of cofactors. Examples of Pou1f1 interactions include the  
59 association with Pitx1 *via* the Pou1f1-TAD to activate the *Prl* and *Gh* promoters (7), and association  
60 with the LIM domains of Lhx3 through the Pou1f1-homeodomain to activate the *Pou1f1*, *Tsh $\beta$*  and *Prl*  
61 promoters (8, 9) as well as the human *PRL* promoter (9). Importantly, forced co-expression of Pou1f1  
62 along with ELK1 (an ubiquitous transcription factor) is capable of activating the endogenous *GHI* in  
63 the human HEK293 cell line to levels 23-fold greater than measured in the non-transfected cells (10).  
64 These studies highlight the central and essential functions of POU1F1 in anterior pituitary  
65 development and in corresponding expression of three landmark hormones, GH, PRL and TSH $\beta$ .

66 Naturally occurring mutations in *Pou1f1* were initially reported in the Snell and Jackson mice,  
67 two dwarf strains with combined deficits in Gh, Tsh $\beta$  and Prl associated with a hypoplastic anterior  
68 pituitary (11). In humans, the first *POU1F1* mutations were identified in 1992 (12) and 35 distinct  
69 mutations have since been reported worldwide (HGMD: hgmd.cf.ac.uk). The vast majority of these  
70 mutations act in a recessive manner with only six demonstrating an autosomal dominant inheritance of  
71 hormone deficiency. Although the detailed clinical attributes of patients with the various *POU1F1*

72 mutations can vary, these patients consistently display an overall picture of combined pituitary  
73 hormone deficiency (CPHD) of GH, PRL, and TSH. GH and PRL deficiencies in affected individuals  
74 are initially noted early in childhood, whereas the central hypothyroidism tends to appear later in  
75 childhood or in adolescence. Radiologic imaging in these individuals often reveals a small anterior  
76 pituitary gland with a normal posterior pituitary and infundibulum.

77         The human growth hormone cluster contains five genes; *GHI* is expressed specifically in the  
78 pituitary somatotropes while the expression of its four paralogs, *GHV*, *CSA*, *CSB*, and *CSL* (a  
79 pseudogene), is specific to the syncytiotrophoblast epithelium lining the placental villi. This multigene  
80 locus contrasts with the single *Gh* gene locus in the mouse. It was generated by local duplications of  
81 the ancestral *GH* gene at a point subsequent to the divergence of the rodent and primate lineages. The  
82 *GHI* promoter contains a pair of conserved POU1F1 binding sites within its proximal 200-bp region.  
83 In humans, these two sites (hereafter named prox-*GHI* and prox-*GH2*) are not sufficient for high-level  
84 expression of *GHI* in the pituitary when assayed in mouse transgenic assays (13). Instead, a powerful  
85 enhancer, HSI, located 14.5 kb 5' to the *hGHI* promoter, is both necessary and sufficient to drive high  
86 levels of *GHI* in the somatotrope. This HSI enhancer is a component of the *hGH* locus control region  
87 (LCR) and does not appear to have a correlate in the mouse genome. HSI contains a tightly packed  
88 array of three POU1F1 binding sites (*HSI-A*, *HSI-B* and *HSI-C*). These three sites play an essential  
89 role in both the activation and the maintenance of *hGHI* transcription in the somatotrope (14–17) and  
90 in its maintenance in the adult (18). POU1F1 binding at these LCR sites within HSI triggers the  
91 formation of an extensive (32kb) domain of histone acetylation throughout the *hGH* locus (19) and is  
92 essential for bringing the LCR in close proximity (“looping”) to the *hGHI* promoter (20–22). It has  
93 been demonstrated that a single base difference between POU1F1 binding sites at the *hGHI* promoter  
94 and those at HSI modifies the conformation of the POU1F1/DNA complex suggesting that these  
95 complexes may function through differential cofactor recruitment (23). Thus POU1F1 appears to have  
96 distinct functions in binding to its cognate sites at HSI and within the *hGHI* promoter.

97         Here we describe a family in which nine members in three generations manifest growth  
98 retardation linked to isolated growth hormone deficiency (IGHD). These individuals lack evidence for  
99 associated TSH and PRL deficiency. This phenotype was inherited in an autosomal dominant pattern

100 and co-segregated over three generations with a missense mutation within the POU1F1 transcriptional  
101 activation domain. A series of *in vitro* and *in vivo* functional assays were carried out to delineate the  
102 mechanism(s) underlying this novel dominantly-inherited isolated GH deficit.

## 103 **Results**

### 104 **Identification of a short stature phenotype inherited in an autosomal dominant pattern over** 105 **three generations of a human kindred**

106         Nine individuals (5 females and 4 males) from the same non-consanguineous Caucasian  
107 family originating from the east of France demonstrated findings of severe growth retardation. The  
108 short stature phenotype segregated as an autosomal dominant trait over three successive generations.  
109 Height standard deviation (SD) scores, at the time of diagnosis, varied from -3 to -5.4 (Fig. 1A) and all  
110 patients had a serum GH peak below 5µg/L (Table 1). The endocrine deficit was limited to a  
111 deficiency in growth hormone (i.e. IGHD phenotype) (Table 1). Although basal serum PRL was  
112 relatively low in affected individual III.7, the TRH stimulation induced a five-fold increase suggesting  
113 that PRL expression and regulation was not adversely affected. Eight of the affected individuals (II.2,  
114 II.4, II.6, II.8, II.10, III.1, III.4 and III.7) benefited from a GH treatment with significant augmentation  
115 in linear growth (the 9<sup>th</sup> individual, I.2, was not treated due to advanced age).

116         Magnetic resonance imaging (MRI) of the pituitary region performed in three affected  
117 members of the family was found to be normal in one case (III.7) and showed anterior pituitary  
118 hypoplasia for two individuals (III.1 and III.4); no abnormalities at the level of posterior pituitary,  
119 pituitary stalk, septum pellucidum, corpus callosum or optic nerves were detected. These data allowed  
120 us to conclude that a mutation resident in this kindred resulted in an isolated GH deficiency  
121 segregating as an autosomal dominant trait.

### 122 **Affected individuals in the kindred carry a novel mutation at the *POU1F1* locus**

123         The low levels of *hGHI* expression in the 9 short stature individuals and the hypoplasia of the  
124 anterior pituitary in 2 of 3 studied, prompted us to screen for mutations in a defined set of genes  
125 critical to GH synthesis and/or pituitary development; *GHI*, *LCR-GHI* (*HSI* fragment), *GHRHR*,

126 *GHRH*, *GHSR*, *GHRL* and *HESX1* genes (see Methods for details). The sequence of each of these  
127 target genes was normal. Causes of developmental defects of the pituitary were next assayed by  
128 analysis of the *PROPI* and *POU1F1* genes in individual III.4. While *PROPI* analysis revealed a  
129 normal sequence, the analysis of *POU1F1* revealed heterozygosity for a sequence variant in exon 3,  
130 c.227C>T (Fig. 1B). This base transition, not previously described in ExAC (exac.broadinstitute.org)  
131 or in Ensembl (ensembl.org), results in a non-conservative substitution that replaces Proline by  
132 Leucine at codon 76. This Pro76Leu (P76L) substitution maps within the highly conserved  
133 transcriptional activation domain (TAD) and involves a proline residue that is invariant in vertebrates  
134 spanning evolution from zebrafish to primates (Figs. 1C, 1D). To establish its intra-familial  
135 segregation, the region of the *POU1F1* gene encompassing the mutation (exon 3) was subsequently  
136 sequenced in all available family members. This analysis revealed a perfect segregation of the defined  
137 mutation with the short stature phenotype (Fig. 1A). These data lead us to conclude that the  
138 dominantly inherited IGHD in this family was due to the defined c.227C>T at the *POU1F1* locus.

#### 139 **Nuclear localization of the POU1F1 transcription factor is unaffected by the P76L mutation**

140 To assess the functional consequences of the P76L mutation at the protein level, we first  
141 assessed the subcellular distribution of the mutant POU1F1 protein. Expression plasmids encoding HA  
142 tagged versions of the WT and the P76L POU1F1 proteins (pcDNA4-POU1F1\_WT-HA and  
143 pcDNA4-POU1F1\_P76L-HA, respectively) were individually transfected into the human embryonic  
144 kidney cell line, HEK293T. Protein accumulation was assessed in individual cells by  
145 immunofluorescence microscopy with an anti-HA antibody (Fig. 2A). The analyses of both the WT  
146 and the mutant POU1F1 proteins revealed intense nuclear staining. These data suggest that the  
147 mutation fails to alter the nuclear import and retention of POU1F1.

#### 148 **The P76L POU1F1 mutation has a negative impact on transcriptional activation of the GH gene**

149 The functional impact of the P76L mutation on POU1F1 transcriptional activity was assessed  
150 in a luciferase reporter assay. The luciferase ORF was placed under the transcriptional control of the  
151 *hGH1* promoter (containing two well described POU1F1 binding sites) linked to the 404-bp HSI  
152 fragment of the *hGH* LCR encompassing an array of three critical POU1F1 binding sites (Fig. 2B,

153 top). The reporter plasmid was co-transfected into HEK293T cells along with a plasmid expressing the  
154 WT or the P76L POU1F1 protein. Western analysis of three independent studies revealed that the  
155 mutant protein was expressed at levels equal to or greater than the WT POU1F1 (Fig 2B and data not  
156 shown). The co-transfection with the WT POU1F1 protein increased luciferase reporter activity by 5-  
157 fold over that of an empty vector. The transcriptional enhancement of the luciferase reporter by the  
158 P76L POU1F1 was 50% relative to the WT (Fig 2B). It was additionally noted that co-transfection of  
159 equal amounts of the plasmid encoding the POU1F1 proteins did not inhibit the transcriptional activity  
160 associated with the wild-type POU1F1 protein (Fig 2C). These data lead us to conclude that the P76L  
161 POU1F1 mutation results in a decrease in transcriptional activity of the *GH* gene, but argue against a  
162 dominant effect of the mutant protein, at least in the context of defined reporter assay.

163 **POU1F1\_P76L has a differential impact on POU1F1 binding to cognate sites at HSI of the *hGH***  
164 **LCR and at the *GHI* promoter**

165 The decreased transcriptional capability of POU1F1\_P76L prompted us to compare the  
166 binding affinity of the WT and mutant POU1F1 protein towards a subset of cognate binding targets.  
167 This was done by subjecting bacterially generated WT and P76L POU1F1 proteins to surface plasmon  
168 resonance (SPR) analysis. For purposes of the analysis, the WT and mutant proteins were generated in  
169 parallel with all culture and purification steps held constant. Of note, we observed a 40-fold higher  
170 recombinant protein yield from the bacterial cultures expressing the WT vs the mutant protein. This  
171 difference appeared to reflect the formation of inclusion bodies in cultures of the mutant protein  
172 because the yield of the mutant protein was increased by culturing at lower temperature. This  
173 difference in solubility is consistent with an altered conformation of the POU1F1\_P76L protein.  
174 Biotinylated DNA targets representing the defined POU1F1 binding sites of the *hGHI* promoter and of  
175 HSI were immobilized on a streptavidin (SA) sensor chip and used for the analysis.

176 For a first qualitative test, equal amounts of the purified recombinant POU1F1\_WT and  
177 POU1F1\_P76L proteins (quantified by Experion; see Methods) were then loaded as analytes. The  
178 recorded resonance units (RU) showed that the WT and P76L POU1F1 proteins bind the promoter and  
179 the HSI DNA targets; the difference of 11RU on HSI target is significant. This result allows us to



180 conclude that POU1F1\_P76L binds better than POU1F1\_WT at the same concentration under our  
181 assay conditions (Fig. 3A). As a control, we performed similar experiments with a recombinant form  
182 of POU1F1 carrying a previously identified CPHD missense mutation (24). This mutation in a  
183 conserved residue of the homeodomain abolishes the binding of POU1F1 to its DNA targets  
184 demonstrated by a dramatic loss of binding in our SPR analysis (Fig 3A).

185 We next evaluated the affinity of the WT and the P76L proteins for their DNA targets in a set  
186 of kinetic binding studies (see Methods). The dissociation constants obtained on the *GHI* promoter  
187 measured using various concentrations of those proteins were similar for the POU1F1\_WT and the  
188 POU1F1\_P76L proteins ( $K_d$  of  $1.7 \times 10^{-8} \text{M}$  and  $2.4 \times 10^{-8} \text{M}$ , respectively) (Fig. 3B, right panel). In  
189 contrast, the  $K_d$  of the POU1F1\_P76L protein was significantly lower than that of the wild-type  
190 protein (i.e.  $2.0 \times 10^{-7} \text{M}$  vs  $2.0 \times 10^{-6} \text{M}$ ) when tested for interaction with *HSI* (Fig. 3B, left panel). This  
191 increased affinity of the POU1F1\_P76L protein for the *HSI* sites was linked to an increased  
192 association rate:  $k_a = 5.9 \times 10^2 \text{ mole}^{-1} \text{ s}^{-1}$  for the POU1F1\_WT and  $k_a = 3.0 \times 10^3 \text{ mole}^{-1} \text{ s}^{-1}$  for the  
193 POU1F1\_P76L protein. These kinetic studies show that the WT POU1F1 protein has higher affinity  
194 on the promoter sites than on the *HSI* sites. These data lead us to conclude that the P76L mutation has  
195 a differential impact on the interaction of the POU1F1 protein with different sets of cognate binding  
196 sites.

### 197 **POU1F1\_P76L alters the binding of the POU1F1 WT protein at cognate sites in the *GHI* but not** 198 ***PRL* promoter**

199 We next compared by EMSA the binding of the WT alone, the POU1F1\_P76L alone, and a  
200 mix of the two proteins, as would occur in individuals heterozygous for the P76L mutation. Binding  
201 was assessed for DNA fragments containing the full set of POU1F1 binding sites (*HSI* and *GHI*  
202 promoter) or each of the corresponding individual POU1F1 binding sites (*HSI*-A,B,C and prox-GH1,  
203 prox-GH2). Remarkably, the migration patterns were different for the DNA incubated with  
204 POU1F1\_WT (lane 2), POU1F1\_P76L (lane 3) and the mix of these two proteins (lane 4) for the *HSI*  
205 (Fig. 4A-D) and for the *hGHI* promoter sites (Fig. 4E-G). These data suggest a modified binding  
206 conformation of the WT/mutant dimer (POU1F1\_WT/POU1F1\_P76L) complex on all POU1F1

207 binding sites of the *GHI* promoter and HSI. Of note, the POU1F1\_WT/POU1F1\_P76L mix showed the  
208 same migration pattern as POU1F1\_WT when assayed for binding to the prolactin promoter (i.e. *PRL-1*  
209 *1* and *PRL-2*) (Fig. 4H, I). These data are consistent with the disease phenotype characterized by a  
210 deficit in GH with no PRL deficiency.

### 211 **The P76L mutation increases the interaction of POU1F1 with three different POU1F1** 212 **transcriptional cofactors**

213 The impact of the POU1F1 mutation on complex formation with two pituitary-specific (PITX1  
214 and LHX3a) transcriptional cofactors and one ubiquitous transcription factor (ELK1) was assessed by  
215 co-immunoprecipitations after cotransfection in HEK293T cells of an expression plasmid encoding the  
216 HA-tagged POU1F1\_WT or POU1F1\_P76L with a plasmid encoding PITX1, LHX3a or ELK1.  
217 Nuclear proteins were immunoprecipitated with an anti-HA antibody and the pellets were  
218 subsequently assayed for each cofactor by western blot (Fig. 5, left panel). In parallel the nuclear  
219 proteins were also immunoprecipitated with antibodies directed against each cofactor and the western  
220 blots were revealed with an anti-HA-antibody (Fig. 5, right panel). The data revealed that the P76L  
221 mutation enhances complex formation with each partner by 5 - 10 folds when compared to the WT  
222 POU1F1 protein (Fig. 5A, 5B, 5C). A formal possibility is that the difference in amount of complex  
223 observed is due to the POU1F1\_P76L conformational difference which would make the protein  
224 complex more accessible the HA-tag to antibody. Co-immunoprecipitations performed with antibodies  
225 directed against each of the interacting proteins allowed us to rule out this possibility.

226 To further evaluate the importance of the peptide surrounding Pro76 in these interactions, we  
227 performed similar co-immunoprecipitation experiments with different POU1F1 mutants in which  
228 Pro76 and the neighboring (Leu74, Thr75, Cys77 and Leu78) were each individually replaced by  
229 alanine residues. The amount of complex formed with PITX1 and LHX3a (Fig. 6A and 6B,  
230 respectively) was increased most prominently by the P76A and P76L substitutions. Moreover, with  
231 ELK1 cofactor (Fig. 6C), the leucine substitution seemed to have a critical impact since an alanine did  
232 not modify the amount of complex formed. These data demonstrate a major role of the Pro76 residue  
233 in the interaction of the POU1F1 trans-activating domain with at least three partners.

234 **A mouse model of the P76L mutation confirms the adverse impact on gene expression but fails**  
235 **to recapitulate the dominant inheritance pattern**

236 To study the functional consequences of the P76L mutation in an *in vivo* context, we  
237 introduced the P76L mutation into the mouse *Pou1f1* locus (see Methods and Fig. 7A). The expression  
238 of P76L encoding *Pou1f1* mRNA was confirmed in the pituitaries of P76L/wt mice and the mRNA  
239 from the mutant allele was shown to be expressed at equivalent levels to the WT allele by a  
240 comparative RT/PCR (Fig. 7B). Remarkably, however, the expression of the mutant Pou1f1\_P76L  
241 protein was markedly suppressed, with steady state levels in the mouse pituitary less than 10% of  
242 output from the endogenous WT locus (Fig. 7C, asterisk). The expression of mRNA from each of three  
243 endogenous Pou1f1-dependent genes (*mGh*, *mPrl*, *mTsh*) were assessed and found to be unaltered in  
244 mice heterozygous for the P76L mutation (data not shown). Similarly, the expression of the *hGH1*  
245 gene from the *hGH/BAC* transgene in the P76L heterozygous mouse was expressed at normal levels  
246 (data not shown). Consistent with the low level expression of Pou1f1 from the mutant locus, mice  
247 homozygous for the P76L mutation displayed a dwarf phenotype (Fig. 7D). Overall, these data point  
248 to a defect in steady state expression of the P76L mutant Pou1f1 protein. This deficiency in protein  
249 expression is consistent with the poor yield of recombinant protein in the bacterial cultures and may  
250 reflect a major alteration in protein solubility or stability *in vivo*.

251 **Discussion**

252 POU1F1 is essential for the formation of the somatotrope, lactotrope, and a subset of the  
253 thyrotrope lineages. As such, all *POU1F1* mutations thus far reported are linked to combined pituitary  
254 hormone deficiency (CPHD) comprising decreases in expression of GH, PRL and TSH (25). In the  
255 current study, we report the first example of a *POU1F1* mutation that is linked to an isolated GH  
256 deficiency. Functional data reveal that the P76L mutation, located in a highly conserved segment of  
257 the transcriptional activation domain (TAD), impacts on the binding patterns of POU1F1 and on the  
258 interaction of POU1F1 with protein partners. The predicted conformational change induced by the  
259 non-conservative substitution of a proline for a leucine is consistent with the low steady state levels of

260 the mutant protein in the mouse despite normal levels of mRNA synthesis. Thus the P76L missense  
261 mutation results in an unusual situation: a specific disruption of the human *GHI* gene expression.

262 Several lines of evidence demonstrate that the P76L variation identified in POU1F1 is a  
263 disease-causing mutation. First, the strict co-segregation of the phenotype with this mutation in 9  
264 individuals over 3 generations. Second, the transcriptional activity of the POU1F1\_P76L on the  
265 chimeric *LCR-hGH* promoter is significantly lower than that of POU1F1\_WT. Third, using SPR  
266 assays, we show that the P76L mutation leads to an increased affinity of POU1F1 for the LCR sites.  
267 Fourth, bandshift assays reveal that the DNA binding pattern of a mix of POU1F1\_WT and  
268 POU1F1\_P76L is different from that of POU1F1\_WT alone on all five cognate binding sites in the  
269 *hGH LCR* and *GHI* promoter but not on the two cognate sites in the *PRL* binding sites. Fifth, as  
270 shown by co-immunoprecipitation studies, the P76L mutation increases the interaction of POU1F1  
271 with three of its known cofactors: PITX1, LHX3a and ELK1.

272 A predicted impact of the POU1F1\_P76L mutation on conformation is consistent with the  
273 noted low yield of the mutant protein compared to the WT protein in two distinct settings; in *E. Coli*  
274 and in mice carrying the heterozygous *Pou1f1* mutation. It should be noted, however, as a formal  
275 possibility that the low protein expression in the mouse model may be contributed to by the presence  
276 of the myc epitope tag which was present at the mutant locus but not at the wt *Pou1f1* locus.

277 Noteworthy, two additional missense mutations have been identified in the human POU1F1  
278 TAD, P14L (26) and P24L (27). Both of these mutations result in a dominantly inherited form of  
279 pituitary deficit. However, in both cases, the patients displayed a classical CPHD phenotype rather  
280 than the isolated GH loss currently being reported. The mutation site within the TAD, therefore  
281 appears critical in terms of phenotypic consequences. The 3D-structure of the POU1F1 TAD remains  
282 undefined and *in silico* modeling could not be performed to test the relative impacts of the P76L, P14L  
283 and P24L mutations on the three dimensional structure. Of note, however, all three of these constitute  
284 a non-conservative substitution of proline for leucine that is predicted to have a major impact on  
285 protein secondary structure and tertiary folding.

286 Our attempt to model the P76L mutation in the mouse was informative in a number of  
287 respects. This mutation once introduced into the mouse *Pou1f1* locus had no adverse effect on the

288 level of mRNA generated from the locus. Notably however, the steady level of mutant protein  
289 expressed from the P76L locus was markedly suppressed. Mice heterozygous for the mutation had no  
290 appreciable decrease in size while mice homozygous were markedly dwarfed. Thus this mutation  
291 results in a recessive dwarf phenotype in the mouse rather than the dominantly inherited phenotype in  
292 the human kindred, for which, haploinsufficiency cannot be the mechanism underlying the dominant  
293 expression of the disease phenotype since the heterozygous parents of patients with homozygous  
294 *POU1F1* null mutation have a normal phenotype. Our *in vitro* data on the coexpression of the mutant  
295 and wild-type POU1F1 proteins argue against a dominant negative effect of the mutant protein over  
296 the wild-type.

297         The data favors a hypothesis of a toxic gain of function associated with the P76L mutation in  
298 humans for two reasons. First, the POU1F1\_P76L protein binds the *LCR* sites with an increased  
299 affinity, as compared to POU1F1\_WT; this affinity difference might disrupt POU1F1\_WT DNA  
300 binding at the *LCR* target sites in heterozygous patients. It is therefore tempting to speculate that the  
301 mutation could result in a higher occupancy at *hGH LCR* target sites precluding the binding of  
302 POU1F1\_WT. Second, we observed that the P76L mutation increases the interactions with three  
303 different cofactors. The mutant protein might therefore titrate POU1F1-interacting proteins leading to  
304 a competition with the wild-type POU1F1 protein. Moreover, co-immunoprecipitation-alanine-  
305 scanning experiments revealed that the amino acid 76 precisely is critical for these interactions; the  
306 weak equilibrium of the *hGHI* transcriptional complex should be modified through the ability to  
307 recruit somatotrope specific cofactors necessary for high *GHI* transcriptional level. Our data in  
308 bandshift assays on the *PRL* promoter target sites are fully in accordance with the phenotype of the  
309 patients with the P76L mutation who had no prolactin deficiency.

310         Of particular interest is the finding that the POU1F1\_WT binds more tightly to promoter sites  
311 than those within the *LCR*. Previous studies have demonstrated that POU1F1 occupies its cognate sites  
312 in the *hGHI* promoter and at HSI of the *hGH LCR* with distinct conformations reflecting a single base  
313 pair difference (23). Thus the missense mutation at position 76 could differentially impact on POU1F1  
314 actions at the *hGH* promoter *via* alterations of HSI function. Such alterations could explain the specific  
315 impact of the mutation on the human *hGH* gene as the *mGh* gene is lacking the HSI enhancer and the

316 *PRL* the *TSH $\beta$*  and the *POU1F1* genes are not known to have corresponding LCR control  
317 determinants.

318 In conclusion, the P76L mutation, which segregates perfectly with the severe growth  
319 retardation, involves a conformation modification of the POU1F1 protein that affects cofactors and  
320 DNA interactions that impact specifically the *hGHI* transcriptional level of expression. This  
321 constitutes a novel mechanism underlying a dominant form of IGHD in humans, also suggesting that  
322 *POU1F1* gene should be screened for this phenotype.

323

## 324 **Materials and methods**

### 325 **Patients**

326 All individuals studied in the reported kindred provided their written informed consent to perform  
327 genetic studies. All were referred to the pediatric endocrinology outpatient clinic of the Nancy  
328 Medical School hospital (CHU of Nancy). Clinical details were assessed using an information sheet  
329 established by our laboratory.

### 330 **Hormonal investigations and magnetic resonance imaging (MRI)**

331 GH plasma values were evaluated after pharmacological stimulations by arginine and ornithine, prolactin  
332 level before and after TRH stimulation, total and free T4 levels, all were measured according to  
333 methods at the time of diagnosis. Pituitary MRI was performed on a 0.5T General Electrics MR max  
334 instrument.

### 335 **Mutation search**

336 Genomic DNA was isolated from blood samples obtained from each individual using standard  
337 technique. All coding exons and intron-exon boundaries of the *GHI*, *LCR-GHI* (AF\_010280),  
338 *GHRHR*, *GHRH*, *GHSR*, *GHRL*, *HESX1*, *PROPI* and *POU1F1* (NM\_000306) genes were amplified  
339 using sets of primers available on request. Sequences were performed according to the thermal cycle  
340 sequencing Big dye terminator protocol (ABI Prism 310 Genetic Analyser, PerkinElmer Applied  
341 Biosystems).

## 342 **Plasmid constructs**

343 The full-length *POU1F1*, and *LHX3a* cDNAs (9) were subcloned into the pcDNA4 or pcDNA3  
344 expression vectors in which HA or Flag tags were inserted in C-terminal, respectively. The *PITX1*  
345 cDNA, amplified from pituitary cDNA (Clontech), was cloned into pcDNA3. The *ELK1* cDNA was  
346 subcloned from pCGN-ELK1 (Addgene, 27156) into pcDNA3 containing a tag Flag in C-terminal.  
347 The QuikChange Site-Directed Mutagenesis Kit (Stratagene) was used to generate plasmids encoding  
348 different POU1F1 mutants, pcDNA4-POU1F1-HA-(P76L, L74A, T75A, P76A, C77A, L78A).  
349 The luciferase reporter plasmid was constructed as follows: 406bp of the *LCR* (HSI, including the  
350 three POU1F1 target sites, AF\_010280) and 494bp of the promoter (including the two POU1F1  
351 binding sites) were linked after amplification using compatible restriction enzyme sites and subcloned  
352 into the pGL3-basic-Luciferase plasmid (Promega) to obtain pGL3-chimer[LCR-promGH] plasmid  
353 (Fig. 2B).

## 354 **Cell culture and transfection**

355 HEK293T cells, obtained from the American Type Culture Collection (Manassas, VA), were grown at  
356 37°C in DMEM (Invitrogen), with 10% fetal calf serum. All transfections were performed at 60%  
357 confluence using the Fugene method (Promega) according to the manufacturer's protocol.

## 358 **Luciferase activity assays and western blot**

359 HEK293T cell extracts were prepared and assayed for luciferase activity, using the Promega assay  
360 system, 48h after co-transfection of the pGL3-chimer[LCR-promGH] reporter gene (100ng) together  
361 with either the empty pcDNA3 expression vector and/or the *POU1F1*-cDNA WT and/or mutant  
362 pcDNA4 constructs at different amounts. Each transfection experiment was carried out in triplicate  
363 and was independently replicated at least three times. Cell extracts were separated on a 10%  
364 polyacrylamide gel, then transferred to a nitrocellulose membrane and probed with an anti-POU1F1  
365 polyclonal antibody (sc-16288, Santa Cruz Biotechnology) and an anti- $\alpha$ βtubulin polyclonal antibody  
366 (2148, Cell Signaling).

## 367 **Protein purification**

368 The full-length *POU1F1* cDNA was cloned at the BamHI NotI sites into the pGEX-6P-1 vector (GE  
369 Healthcare) including a PreScission protease site to remove the GST tag. GST-tagged fusion proteins  
370 were produced in the BL21 DE3 star strain of *Escherichia coli* (Invitrogen). After induction for 3 h  
371 with 0.5 mM isopropyl- $\beta$ -d-thiogalactopyranoside at 37°C for the GST-POU1F1\_WT, at 25°C during  
372 4h for the GST-POU1F1\_P76L, at 15°C for 4h for the GST-POU1F1\_R265W, the bacterial pellet was  
373 freeze/thawed 3 times followed by sonication in PBS1X (200 ml/L of culture), 1% Triton X-100,  
374 10% glycerol and 1mg/ml lysozyme and finally clarified by centrifugation at 22.000 $\times$ g for 20 min.  
375 Supernatants were incubated 30mn at room temperature with glutathione-Sepharose beads (GE  
376 Healthcare), then washed 4 folds in PBS1X. The last wash was performed in cleavage buffer (50mM  
377 Tris-HCl pH7.0, 150mM NaCl, 1mM EDTA, 1mM PMSF), then beads were incubated 4h at 4°C with  
378 600 $\mu$ l of PreScission protease (1U/ $\mu$ l, GE Healthcare) in 40ml of a cleavage buffer. Centrifugation of  
379 beads at 500g 15mn at 4°C allowed to collect soluble purified protein which is concentrated on  
380 Corning Spin-X UF 20ml, 10000 MWCO. Two to 5ml of protein were dialyzed in HBS buffer (10mM  
381 HEPES pH7.4, 150mM NaCl, 3 mM EDTA) overnight. All preparations of proteins were checked on  
382 Experion (BioRad) instrument for their quality and quantification.

### 383 **Surface Plasmon Resonance analysis**

384 Real-time DNA-protein interaction assays were performed using a Biacore 3000 instrument controlled  
385 by Biacore 3000 Control Software v4.1 (GE Healthcare). All experiments were done at 25°C. After  
386 preincubation in 1M NaCl, 50mM NaOH for 1min (3 times), 75 $\mu$ l of 500nM biotinylated DNA was  
387 covalently coupled to a streptavidine (SA) sensor chip (GE Healthcare) (5 $\mu$ L/min) in HBS-EP running  
388 buffer [10 mM Hepes (pH7.4), 150 mM NaCl, 3 mM EDTA, 0.005% surfactant P20]. The chip was  
389 then washed 1min (5 $\mu$ L/min) with 1M NaCl, 50mM NaOH. Real-time monitoring was displayed in a  
390 sensorgram as the resonance unit (RU) *versus* time (s). The 70-bp fragment of the *GHI* promoter (two  
391 POU1F1 binding sites) was generated by annealing a sense (5' biotinylated) and antisense  
392 oligonucleotide and 900RU were obtained. A 212-bp PCR product corresponding to the *HSI* (three  
393 POU1F1 binding sites) was amplified from genomic DNA using a biotinylated primer and 1900RU  
394 were anchored. Binding studies were performed during 5min with 25 $\mu$ l of 50nM purified protein in



395 HBS-EP, 1mM MgCl<sub>2</sub>. The chip surface was regenerated using 0.1%SDS (flow rate: 30μl/min;  
396 contact time: 30s). Kinetic studies were performed at least in triplicate. Defined concentrations (from 0  
397 to 50nM) of POU1F1 proteins were injected with a 5min association phase and 8min dissociation  
398 phase and their dose dependency response was measured. Data were analysed with BIAevaluation  
399 software 4.1 and the K<sub>d</sub> dissociation constant was determined using the Fit kinetic simultaneous  
400 K<sub>A</sub>/K<sub>D</sub> (1:1 binding; Langmuir algorithm) and validated when the Chi<sup>2</sup> was <10 (this value means that  
401 the model used for fitting adequately describes the data).

#### 402 **Subcellular localization**

403 HEK293T cells were seeded at 50% confluence on a strip into each chamber of a six-chamber tissue  
404 culture plate. After transfection of pcDNA4-POU1F1\_WT-HA or pcDNA4-POU1F1\_P76L-HA, cells  
405 were fixed 24h in 4% paraformaldehyde and permeabilized in PBS1X-Triton 0.1%. Slides were then  
406 blocked with PBS1X-Triton 0.1%-BSA10% and incubated with an anti-HA mouse monoclonal  
407 antibody (Sigma) (1/1000) for 1h. The strips were washed and incubated with the Alexa488-goat anti-  
408 mouse secondary antibody (Invitrogen) (1/2000) for 1h. Nuclear counterstaining was performed with  
409 Vectashield containing 4',6-diamidino-2-phenylindole dihydrochloride (DAPI) (Vector Laboratories).  
410 Immunostaining was then visualized on a Nikon eclipse 80i microscope, and images were captured  
411 using a Qimaging (Retiga 2000R) camera and Image Pro Express 6.0 software.

#### 412 **Co-immunoprecipitation**

413 HEK293T cells (3x10<sup>6</sup>) were transfected with 1.5μg of pcDNA4-POU1F1\_WT-HA or of pcDNA4-  
414 POU1F1\_P76L-HA- plasmids and 1.5μg of one of the plasmid encoding the cofactor tested (pcDNA3-  
415 PITX1, pcDNA3-LHX3a-Flag or pcDNA3-ELK1-Flag). Nuclear extracts prepared after 30h of  
416 expression were divided in two parts and incubated overnight with each antibody, using Universal  
417 magnetic CoIp kit (Active Motif) following manufacturer's instructions. Purified proteins from  
418 magnetic beads were then resolved by SDS-PAGE, immunoblotted, and revealed by  
419 chemiluminescence (Supersignal West Dura Chemiluminescent Substrate, Pierce, Thermo Scientific).  
420 Quantity One 1D analysis software (Bio Rad) was used to visualize and to quantify (Volume

421 Rectangle tool) the complex formed between the two proteins: histograms represent protein  
422 immunoprecipitated/input protein expression ratios.

### 423 **Electrophoretic Mobility Shift Assay (EMSA)**

424 The LightShift Chemiluminescent EMSA kit (Pierce) was used for the study. 20 fmoles of different  
425 Biotin end-labeled DNA duplexes (prom*GHI* 70bp, *HSI* 212bp, prox-*GHI* 32bp, prox-*GHI* 30bp,  
426 *HSI-A* 37bp, *HSI-B* 37bp, *HSI-C* 38bp, *PRL1* (=3P) 29bp, *PRL2* (=1P) 29bp (23) were incubated for  
427 20mn at room temperature with 200ng of POU1F1 purified proteins. The DNA-protein complexes  
428 were subjected to a 5% or 6% native polyacrylamide gel electrophoresis and transferred using the  
429 PierceG2 Fast-blotter system (Thermo-Scientific) to a nylon membrane (Biodyne B, Pierce). After  
430 transfer, the membrane was immediately cross-linked (UV Stratalinker 2400, Stratagene) using  
431 autocrosslink program. A chemiluminescent method utilizing a luminol/enhancer solution and a stable  
432 peroxide solution (Pierce) was used as described by the manufacturer.

### 433 **Mouse model**

434 The P76L mutation was introduced into the mouse genome *via* standard homologous recombination in  
435 mouse ES cells. The recombinant ES cells were validated for the presence of the corresponding  
436 introduced single nucleotide substitution as well as the presence of the Neo<sup>R</sup> selection marker and Myc  
437 epitope tag by direct sequencing of the *Pou1f1* locus of an adult wt/P76L mouse tail DNA. The Neo<sup>R</sup>  
438 cassette, flanked by a unidirectional set of LoxP sites, was deleted by crossing the mouse with a EIIA-  
439 Cre mouse. The final mutant gene was validated by multiple targeted PCR and sequence analyses.

440

### 441 **Acknowledgments**

442 We thank all patients and family members for their cooperation.

443 The work was supported by INSERM

444 **Conflict of interest statement:** none declared

445

446 **References**

- 447 1. Rizzoti,K. (2015) Genetic regulation of murine pituitary development. *J. Mol. Endocrinol.*, **54**,  
448 R55–73.
- 449 2. Andersen,B. and Rosenfeld,M.G. (2001) POU domain factors in the neuroendocrine system: lessons  
450 from developmental biology provide insights into human disease. *Endocr. Rev.*, **22**, 2–35.
- 451 3. Ho,Y., Cooke,N.E. and Liebhaber,S.A. (2015) An autoregulatory pathway establishes the definitive  
452 chromatin conformation at the pit-1 locus. *Mol. Cell. Biol.*, **35**, 1523–1532.
- 453 4. Ingraham,H.A., Flynn,S.E., Voss,J.W., Albert,V.R., Kapiloff,M.S., Wilson,L. and Rosenfeld,M.G.  
454 (1990) The POU-specific domain of Pit-1 is essential for sequence-specific, high affinity  
455 DNA binding and DNA-dependent Pit-1-Pit-1 interactions. *Cell*, **61**, 1021–1033.
- 456 5. Andersen,B. and Rosenfeld,M.G. (1994) Pit-1 determines cell types during development of the  
457 anterior pituitary gland. A model for transcriptional regulation of cell phenotypes in  
458 mammalian organogenesis. *J Biol Chem*, **269**, 29335–8.
- 459 6. Savage,J.J., Yaden,B.C., Kiratipranon,P. and Rhodes,S.J. (2003) Transcriptional control during  
460 mammalian anterior pituitary development. *Gene*, **319**, 1–19.
- 461 7. Szeto,D.P., Ryan,A.K., O’Connell,S.M. and Rosenfeld,M.G. (1996) P-OTX: a PIT-1-interacting  
462 homeodomain factor expressed during anterior pituitary gland development. *Proc. Natl. Acad.*  
463 *Sci. U. S. A.*, **93**, 7706–7710.
- 464 8. Bach,I., Rhodes,S.J., Pearse,R.V., Heinzl,T., Gloss,B., Scully,K.M., Sawchenko,P.E. and  
465 Rosenfeld,M.G. (1995) P-Lim, a LIM homeodomain factor, is expressed during pituitary  
466 organ and cell commitment and synergizes with Pit-1. *Proc Natl Acad Sci U A*, **92**, 2720–4.

- 467 9. Sobrier,M.-L., Brachet,C., Vié-Luton,M.-P., Perez,C., Copin,B., Legendre,M., Heinrichs,C. and  
468 Amselem,S. (2012) Symptomatic heterozygotes and prenatal diagnoses in a  
469 nonconsanguineous family with syndromic combined pituitary hormone deficiency resulting  
470 from two novel LHX3 mutations. *J. Clin. Endocrinol. Metab.*, **97**, E503–509.
- 471 10. Yang,X., Jin,Y. and Cattini,P.A. (2010) Appearance of the pituitary factor Pit-1 increases  
472 chromatin remodeling at hypersensitive site III in the human GH locus. *J. Mol. Endocrinol.*,  
473 **45**, 19–32.
- 474 11. Li,S., Crenshaw,E.B. d, Rawson,E.J., Simmons,D.M., Swanson,L.W. and Rosenfeld,M.G. (1990)  
475 Dwarf locus mutants lacking three pituitary cell types result from mutations in the POU-  
476 domain gene pit-1. *Nature*, **347**, 528–33.
- 477 12. Radovick,S., Nations,M., Du,Y., Berg,L.A., Weintraub,B.D. and Wondisford,F.E. (1992) A  
478 mutation in the POU-homeodomain of Pit-1 responsible for combined pituitary hormone  
479 deficiency. *Science*, **257**, 1115–8.
- 480 13. Jones,B.K., Monks,B.R., Liebhaber,S.A. and Cooke,N.E. (1995) The human growth hormone gene  
481 is regulated by a multicomponent locus control region. *Mol. Cell. Biol.*, **15**, 7010–7021.
- 482 14. Bennani-Baïti,I.M., Asa,S.L., Song,D., Iratni,R., Liebhaber,S.A. and Cooke,N.E. (1998) DNase I-  
483 hypersensitive sites I and II of the human growth hormone locus control region are a major  
484 developmental activator of somatotrope gene expression. *Proc. Natl. Acad. Sci. U. S. A.*, **95**,  
485 10655–10660.
- 486 15. Shewchuk,B.M., Asa,S.L., Cooke,N.E. and Liebhaber,S.A. (1999) Pit-1 binding sites at the  
487 somatotrope-specific DNase I hypersensitive sites I, II of the human growth hormone locus  
488 control region are essential for in vivo hGH-N gene activation. *J. Biol. Chem.*, **274**, 35725–  
489 35733.

- 490 16. Su, Y., Liebhaber, S.A. and Cooke, N.E. (2000) The human growth hormone gene cluster locus  
491 control region supports position-independent pituitary- and placenta-specific expression in the  
492 transgenic mouse. *J. Biol. Chem.*, **275**, 7902–7909.
- 493 17. Fleetwood, M.R., Ho, Y., Cooke, N.E. and Liebhaber, S.A. (2012) DNase I hypersensitive site II of  
494 the human growth hormone locus control region mediates an essential and distinct long-range  
495 enhancer function. *J. Biol. Chem.*, **287**, 25454–25465.
- 496 18. Ho, Y., Shewchuk, B.M., Liebhaber, S.A. and Cooke, N.E. (2013) Distinct chromatin configurations  
497 regulate the initiation and the maintenance of hGH gene expression. *Mol. Cell. Biol.*, **33**,  
498 1723–1734.
- 499 19. Ho, Y., Elefant, F., Cooke, N. and Liebhaber, S. (2002) A defined locus control region determinant  
500 links chromatin domain acetylation with long-range gene activation. *Mol Cell*, **9**, 291–302.
- 501 20. Ho, Y., Tadevosyan, A., Liebhaber, S.A. and Cooke, N.E. (2008) The juxtaposition of a promoter  
502 with a locus control region transcriptional domain activates gene expression. *EMBO Rep.*, **9**,  
503 891–898.
- 504 21. Yoo, E.J., Cooke, N.E. and Liebhaber, S.A. (2012) An RNA-independent linkage of noncoding  
505 transcription to long-range enhancer function. *Mol. Cell. Biol.*, **32**, 2020–2029.
- 506 22. Yoo, E.J., Brown, C.D., Tsai, Y.-C., Cooke, N.E. and Liebhaber, S.A. (2015) Autonomous actions of  
507 the human growth hormone long-range enhancer. *Nucleic Acids Res.*, **43**, 2091–2101.
- 508 23. Shewchuk, B.M., Ho, Y., Liebhaber, S.A. and Cooke, N.E. (2006) A single base difference between  
509 Pit-1 binding sites at the hGH promoter and locus control region specifies distinct Pit-1  
510 conformations and functions. *Mol Cell Biol*, **26**, 6535–46.
- 511 24. Turton, J.P., Strom, M., Langham, S., Dattani, M.T. and Le Tissier, P. (2012) Two novel mutations in  
512 the POU1F1 gene generate null alleles through different mechanisms leading to combined  
513 pituitary hormone deficiency. *Clin. Endocrinol. (Oxf.)*, **76**, 387–393.

- 514 25. Pfäffle,R. and Klammt,J. (2011) Pituitary transcription factors in the aetiology of combined  
515 pituitary hormone deficiency. *Best Pract. Res. Clin. Endocrinol. Metab.*, **25**, 43–60.
- 516 26. Fofanova,O.V., Takamura,N., Kinoshita,E., Yoshimoto,M., Tsuji,Y., Peterkova,V.A.,  
517 Evgrafov,O.V., Dedov,I.I., Goncharov,N.P. and Yamashita,S. (1998) Rarity of PIT1  
518 involvement in children from Russia with combined pituitary hormone deficiency. *Am. J.*  
519 *Med. Genet.*, **77**, 360–365.
- 520 27. Ohta,K., Nobukuni,Y., Mitsubuchi,H., Fujimoto,S., Matsuo,N., Inagaki,H., Endo,F. and Matsuda,I.  
521 (1992) Mutations in the Pit-1 gene in children with combined pituitary hormone deficiency.  
522 *Biochem. Biophys. Res. Commun.*, **189**, 851–855.
- 523

524 **Legends to figures**

525 **Figure 1: Identification of a POU1F1 mutation segregating with a short stature phenotype and**  
526 **low serum GH levels in a three generation kindred**

527 **A.** Genealogical tree of the IGHD family. Squares, males; circles, females; filled black symbols,  
528 IGHD patients. For subjects with growth retardation their height standard deviation (SD) is indicated  
529 between brackets. The genotype (N/N: normal, N/M: heterozygous) is indicated under each tested  
530 individual.

531 **B.** Electrophoregram of the portion of exon 3 showing (black arrow) the heterozygous c.227C>T  
532 transition leading to p.Pro76Leu mutation. The vertical line represents the intron-exon junction.

533 **C.** Schematic representation of the *POU1F1* cDNA and POU1F1 protein: six exons encoding the 291  
534 amino acids protein consisting of two main domains, the Transactivating Domain (TAD, orange) in  
535 which the variation has been identified (noted with an asterisk) and the POU-S and POU-H domains  
536 (homeodomain, purple).

537 **D.** Evolutionary conservation of proline 76 (noted above with an asterisk): interspecies similarity  
538 (shown in one-letter code) of the TAD domain of POU1F1 aligned with sequences of the TAD domain  
539 found in 9 other vertebrates species: black underlined, total conservation; grey underlined,  
540 conservative amino acid substitutions; not underlined, amino acid not conserved and indexed in a  
541 different group.

542 **Figure 2: Conserved nuclear localization and diminished transcriptional activity of the mutant**  
543 **POU1F1 protein**

544 **A.** Subcellular localization of POU1F1\_WT and POU1F1\_P76L in HEK293T cells transfected with  
545 the corresponding HA tagged expression plasmids. 48 hours after transfection, cells were  
546 immunostained with mouse anti-HA antibody (1/1000) then Alexa488 (goat anti-mouse 1/2000).  
547 Nuclei are stained in blue by DAPI. The two proteins (wild-type and mutated) were both localized in  
548 the nucleus. A control with no transfected cells is also shown.

549 **B.** Impact of the Pro76Leu mutation on the transcriptional capability of POU1F1. HEK293T cells  
550 were co-transfected with pcDNA3-POU1F1\_WT-HA or pcDNA3-POU1F1\_P76L-HA in combination

551 with a luciferase reporter ORF under control of the HSI enhancer segment of the *hGH* LCR linked  
 552 directly to the intact *hGH* promoter pGL3-chimer[LCR-promGH]. The previously-defined POU1F1  
 553 binding sites in HSI and in the *hGH* promoter are indicated by the red lines. POU1F1 protein  
 554 expression from the expression vectors was monitored by western blot with anti-POU1F1 polyclonal  
 555 antibody relative to  $\alpha\beta$ tubulin level (top). Luciferase activity represents the means  $\pm$ SD of triplicate  
 556 assays; a representative experiment of three experiments.

557 **C.** Assessment of a potential dominant negative effect of the P76L mutation over the WT protein. Co-  
 558 transfection of the HSI/hGH/Luc reporter with the POU1F1\_WT plasmid, POU1F1\_P76L plasmid in  
 559 increasing amounts up to a saturation response, or with a 1:1 mixture of the two plasmids.

560 **Figure 3: POU1F1 binding to DNA studied by Surface Plasmon Resonance (SPR)**

561 **A.** Sensorgrams. Biotinylated DNAs (*HSI* and *promGHI*) were loaded on a streptavidin chip and  
 562 binding of 50nM of purified WT (blue) or P76L (green) or R265W (red) POU1F1 proteins to the two  
 563 DNA targets was assessed. The recorded resonance units (RU) for each protein were noted.

564 **B.** Kinetics of POU1F1 binding the DNA sites: 0, 10, 20, 30, 40 and 50nM of each purified protein  
 565 were successively loaded on the streptavidin chips on which biotinylated DNA POU1F1 targets have  
 566 been anchored. After data treatment using BIAevaluation software 4.1, the association and  
 567 dissociation constants corresponding to a  $K_d$  value in molar (M) were determined for WT and P76L-  
 568 POU1F1 proteins on each target sequence and represented by histograms: on the *HSI* (left graph) and  
 569 on the *hGHI* promoter (right graph). Each study was performed in triplicate.

570 **Figure 4: Analysis of POU1F1 binding to DNA by electrophoretic mobility shift assays**

571 **A.** 20 fmoles of biotinylated DNA containing a 212-bp segment of HSI encompassing all three  
 572 POU1F1 binding sites (A, B, and C) were incubated with 200ng of purified WT (Lane 2) or mutant  
 573 P76L POU1F1 (Lane 3) protein or with a 1:1 mixture (100ng of each) of the two proteins (Lane 4).  
 574 Lane 1 contains the biotinylated DNA target in the absence of added protein.

575 **B-D.** Binding to each individual POU1F1 binding site within *HSI*. 37bp including one site *HSI-A*, B,  
 576 37bp *HSI-B*, C, 38bp *HSI-C*, D.

577 **E.** Binding to a 70-bp segment of the *GHI* promoter encompassing the two POU1F1 binding sites.



578 **F-G.** Binding to each of the two POU1F1 binding sites in the h*GHI* promoter: 32-bp fragment  
579 encompassing prox-*GHI* (F) or the 30-bp fragment encompassing prox-*GH2* (G).

580 **H-I.** Binding to each of the two POU1F1 binding sites in the human *PRL* gene promoter. 29-bp  
581 fragments containing either *PRL-1* (H) or *PRL-2* (I).

582 **Figure 5: Co-immunoprecipitation of WT and P76L POU1F1 proteins with three cofactors**

583 HEK293T cells were co-transfected with plasmids pcDNA4-POU1F1-HA expressing POU1F1\_WT or  
584 P76L (lanes labeled WT and P76L, respectively) and with each of the following three expression  
585 vectors: pcDNA3-PITX1 (A), pcDNA3-LHX3a-Flag (B) and pcDNA3-ELK1-Flag (C). Nuclear  
586 extracts were co-immunoprecipitated with an anti-HA antibody and the western blots were revealed  
587 with an anti-PITX1 antibody for PITX1 and an anti-Flag antibody for LHX3 and ELK1 (left panels).  
588 The same nuclear extracts were co-immunoprecipitated with an anti-PITX1 antibody for PITX1 and an  
589 anti-Flag antibody for LHX3 and ELK1 and westerns blots revealed with the anti-HA antibody (right  
590 panels); IP: immunoprecipitation, WB: western blots. Quantification of the complex formed,  
591 represented by histograms, was calculated as the ratio of protein immunoprecipitated to protein  
592 expressed (input).

593 **Figure 6: Co-immunoprecipitation POU1F1 with three cofactors. Interactions are compared**  
594 **among the WT POU1F1 and a series of derived alanine substitutions surrounding proline 76**  
595 **site.**

596 HEK293T cells were co-transfected with plasmids pcDNA4-POU1F1-HA expressing POU1F1\_WT or  
597 L74A, T75A, P76L, P76A, C77A, L78A and pcDNA3-PITX1 or pcDNA3-LHX3a-Flag or pcDNA3-  
598 ELK1-Flag. Co-immunoprecipitations were performed with an anti-PITX1 antibody (A) or Flag  
599 antibodies for LHX3a (B) and ELK1 (C) on nuclear extracts samples. Western blots were generated  
600 using an anti-HA antibody. Quantification of the complex formed, represented by histograms (right  
601 side), was evaluated as the ratio of protein immunoprecipitated to protein expressed (input).

602 **Figure 7: Introduction of the P76L mutation into the *Pou1f1* locus in the mouse genome.**

603 **A. Homologous recombination at the *Pou1f1* locus in the mouse genome.** The native *Pou1f1* locus  
604 is shown on the top and the targeting vector used to insert the P76L mutation into the locus is shown  
605 below. The initial recombination product is displayed on the third line and the final locus after  
606 deletion of the Neo<sup>R</sup> cassette *via* Cre/Lox recombination is displayed at the bottom. The position of the  
607 P76L mutation is denoted by the asterisk, the dual selection cassettes, Neo<sup>R</sup> and TK, are represented by  
608 the labeled red rectangles, Lox sites are indicated by the arrowhead, and the positions of the primers  
609 used for selective detection of the wt and mutant *Pou1f1* mRNAs are indicated and numbered below  
610 the diagram.

611 **B. mRNA expression from the PitP76L locus in the mouse pituitary. Top:** *Pou1f1* mRNA  
612 expression from the P76L locus was specifically detected in a mouse heterozygous for the mutant  
613 allele by an RT/PCR assay using a set of primers positioned at exon 2 (primer 1) and within the myc  
614 epitope segment in exon 6 (specific to the mutant allele) (primer 2). **Bottom:** The relative levels of the  
615 mRNA expression from the wt and the mutant locus were directly compared in a mouse heterozygous  
616 for the mutant allele (wt/P76L) and a wt mouse (wt/wt) by an RT/PCR analysis using the exon 5  
617 primer (primer 3) and a primer within the 3' UTR (primer 4) in exon 4, bracketing the myc epitope tag  
618 specific to the mutant locus.

619 **C. Protein expression from the P76L locus in the mouse pituitary.** Western blot of pituitary  
620 extracts from wt/wt and wt/P76L mice were probed with antibodies to mouse Pou1f1 (left blot) and  
621 with an antibody to the myc epitope tag (specific to the mutant locus) (right blot). The overall level of  
622 Pou1f1<sub>WT</sub> protein in the WT/P76L heterozygote pituitary is approximately half of that in the  
623 WT/WT mouse. A faint band at the position of the mutant Pit1 protein (\*) is migrating at the position  
624 predicted from the Pit-1 protein containing the Myc epitope tag. The expression of the P76L Pou1f1  
625 protein was directly verified by re-probing the Western with an antibody to the myc epitope.

626 **D. Growth curves of WT/WT, WT/P76L and P76L/P76L mice.** The body weights are shown in the  
627 Y-axis and the genotypes are indicated for each curve. The analyses of male (top) mice are shown. A  
628 parallel analysis of females gave an identical result (not shown).

629

630

Patient	Height SD	GH	T4	PRL	GH treatment	MRI
<b>I.2</b>	-3.2	Not eval	Not eval	Not eval	-	-
<b>II.2</b>	-4.3	4	<u>70</u>	Not eval	+	-
<b>II.4</b>	-5.4	2.2/2.2	<u>78</u>	Not eval	+	-
<b>II.6</b>	-3	1.5/0.5	<u>58</u>	Not eval, normal breast feeding	+	-
<b>II.8</b>	-4.7	2	<u>94</u>	Not eval	+	-
<b>II.10</b>	-4	3/0.5	<u>10.7</u>	Not eval, normal breast feeding	+	-
<b>III.1</b>	-3.5	4.3/3.1	<u>10.4</u>	3.1 (12.5/TRH)	+	AP hypo
<b>III.4</b>	-3	2.4/2.3	<u>15.2</u>	5.1 (16.7/TRH)	+	AP hypo
<b>III.7</b>	-3.2	2/3.1	<u>11.9</u>	0.9 (4.6/TRH)	+	N

631

632 Table 1 : Clinical and endocrinological data of the nine IGHD patients.

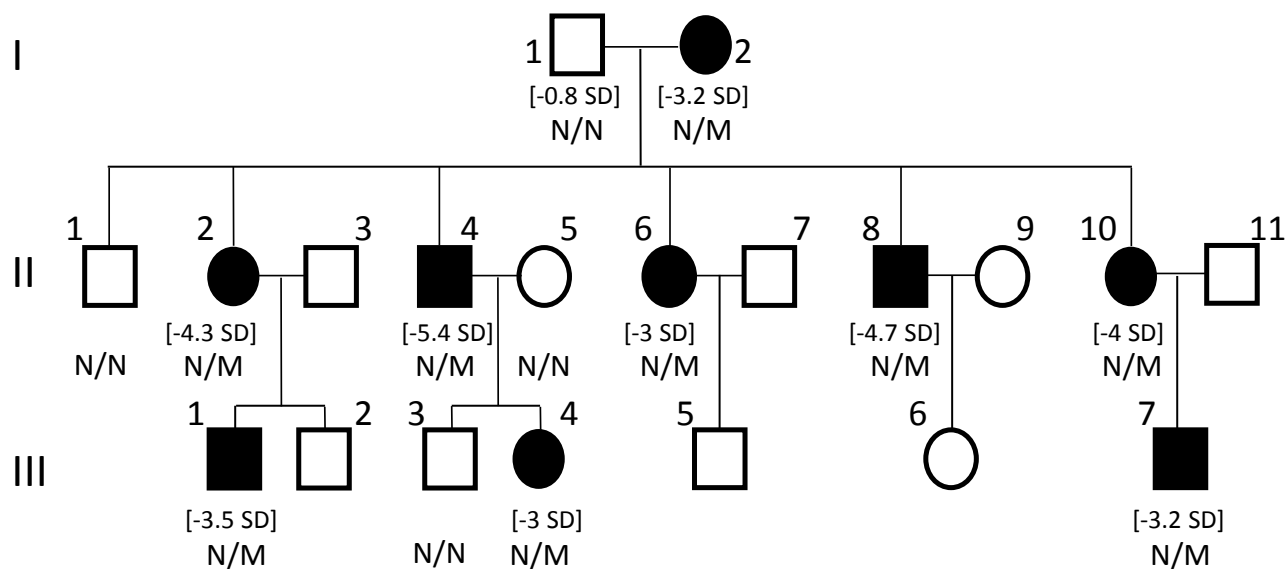
633 Height SD, height standard deviation; GH  $\mu\text{g/L}$ : arginine /ornithine tests, normal value  $>10\mu\text{g/L}$ ; **total**

634 **T4 ng/ml**: normal value 40-120 for II.2, II.4, II.6 and II.8 and free T4 pmole/L normal value 10-21 for

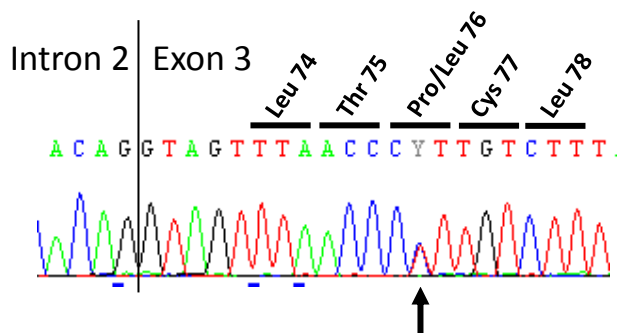
635 II.10, III.1, III.4 and III.7; PRL ng/ml, PRL before and after TRH stimulation (between brackets):

636 normal value 2.5-20. Not eval: not evaluated. AP hypo: hypoplasia of the anterior pituitary, N: normal.

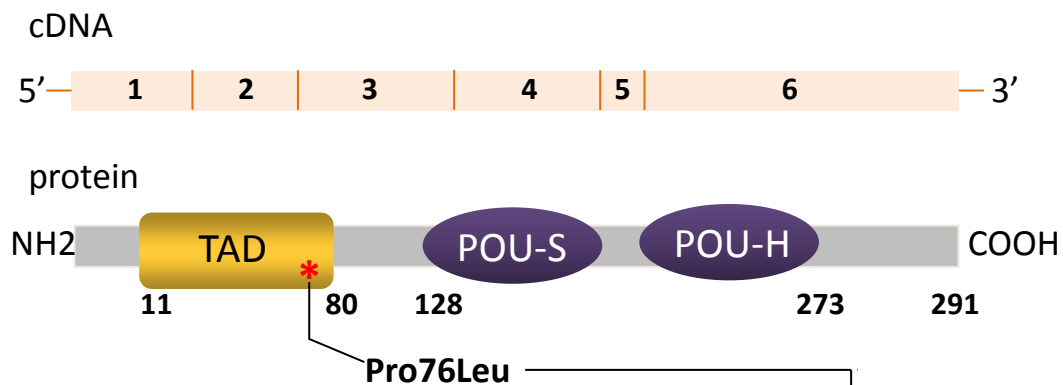
A



B



C



D

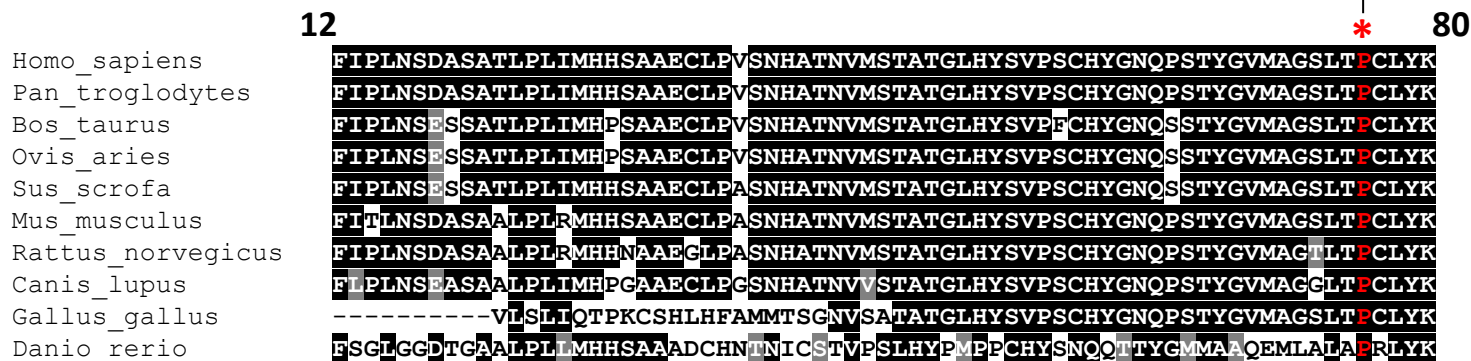
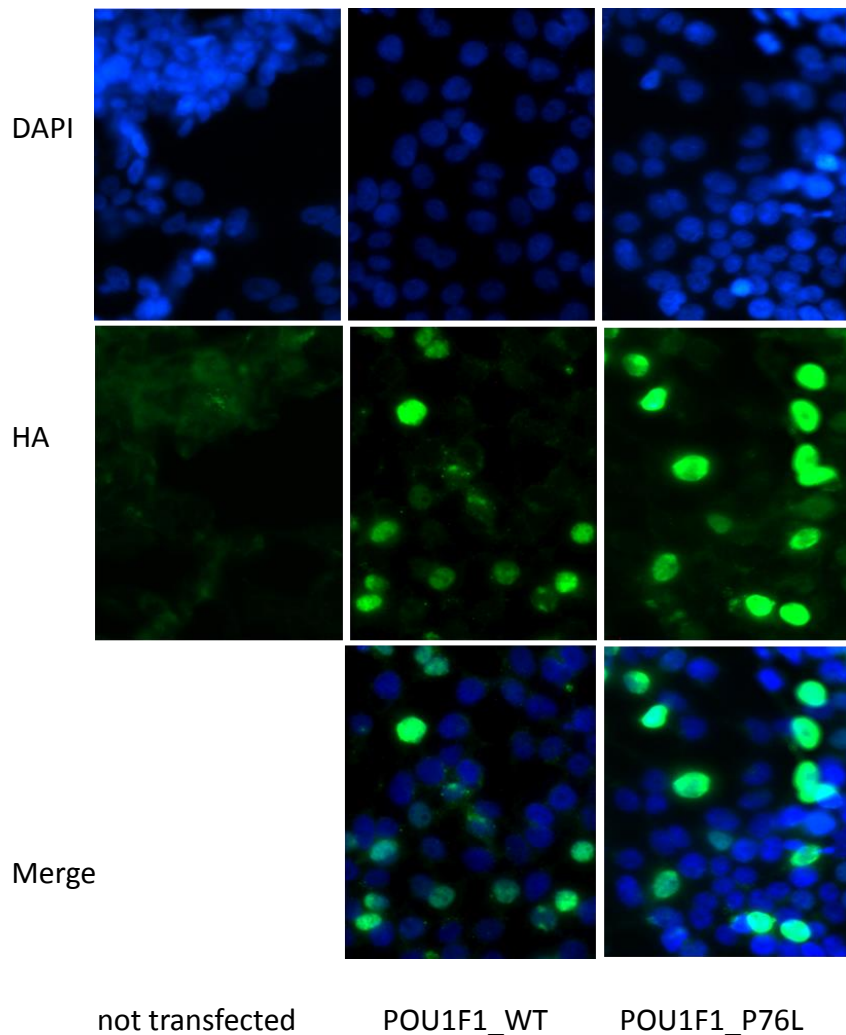
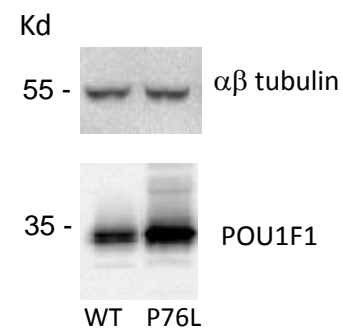
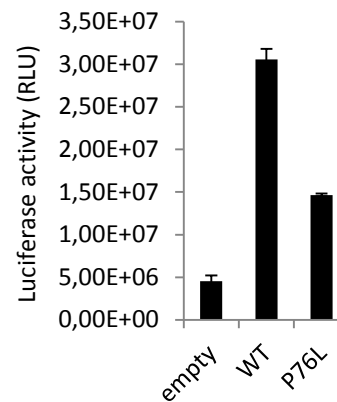
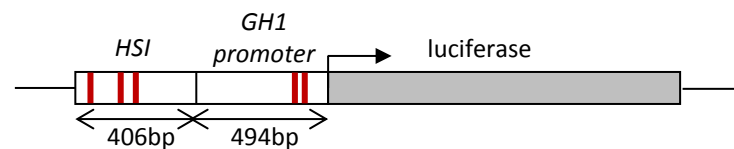


Figure 1

A



B pGL3-chimer[LCR-promGH]



C

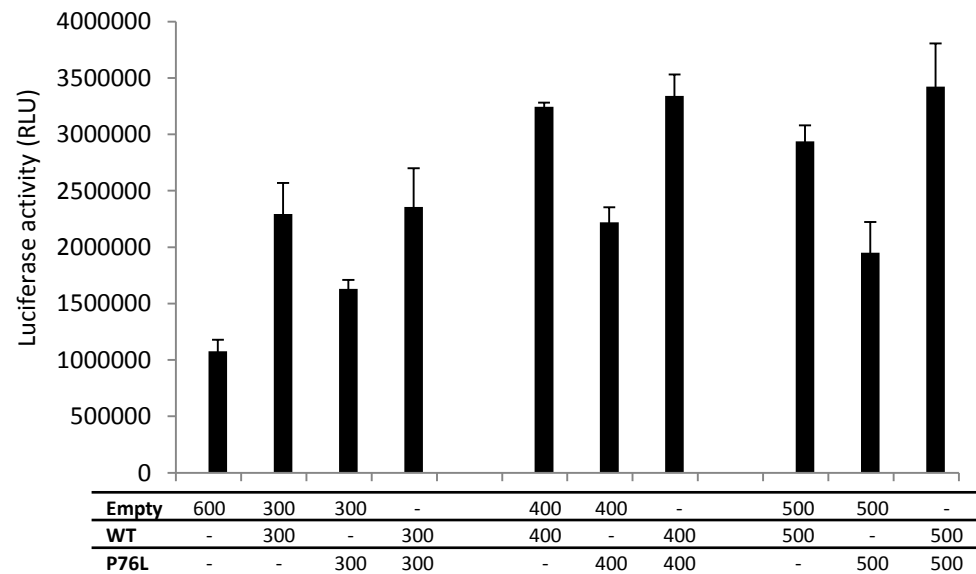
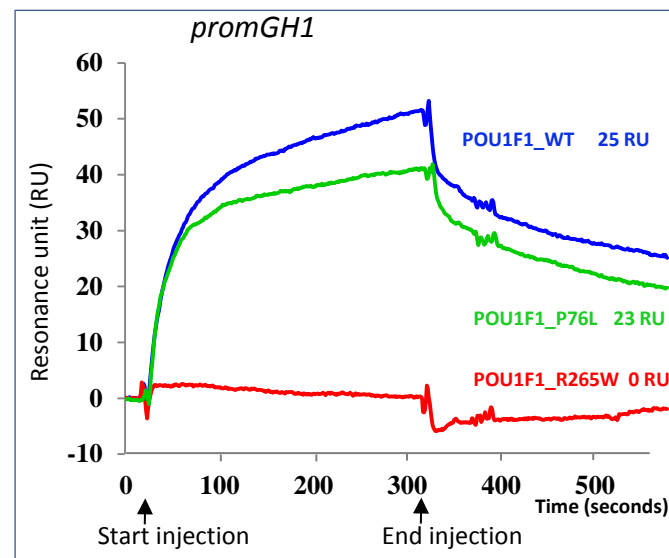
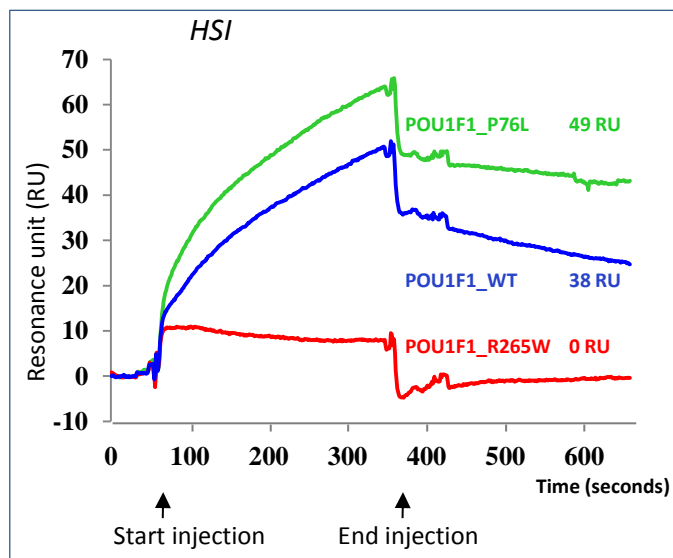


Figure 2

A



B

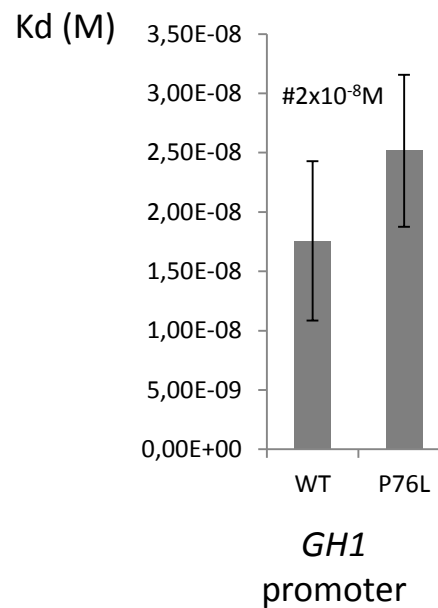
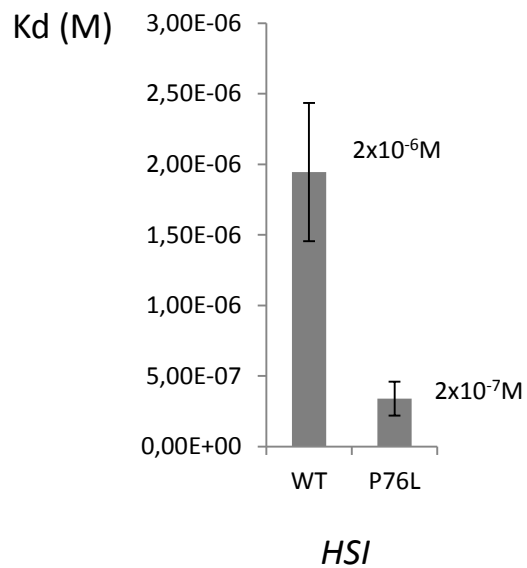


Figure 3

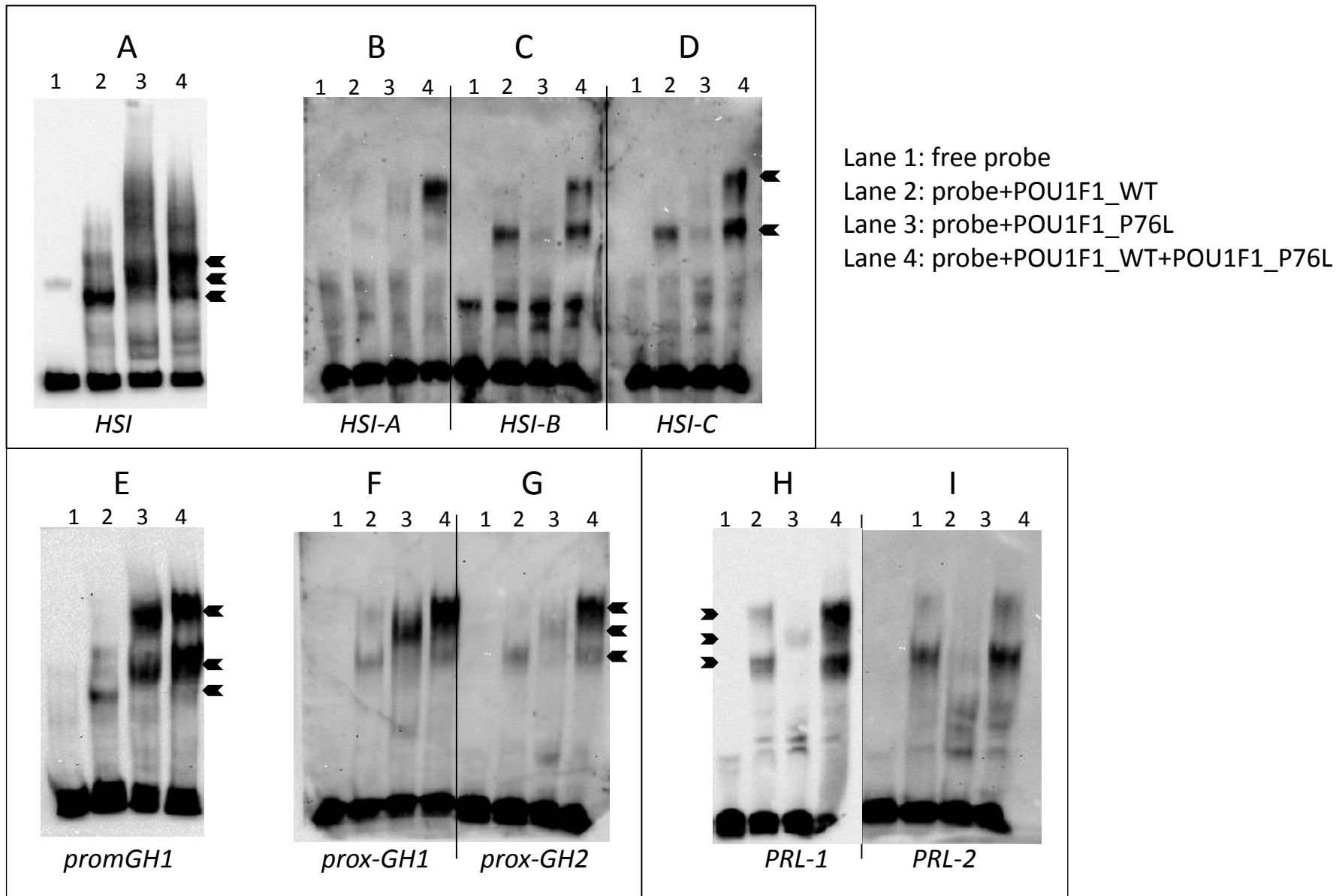


Figure 4

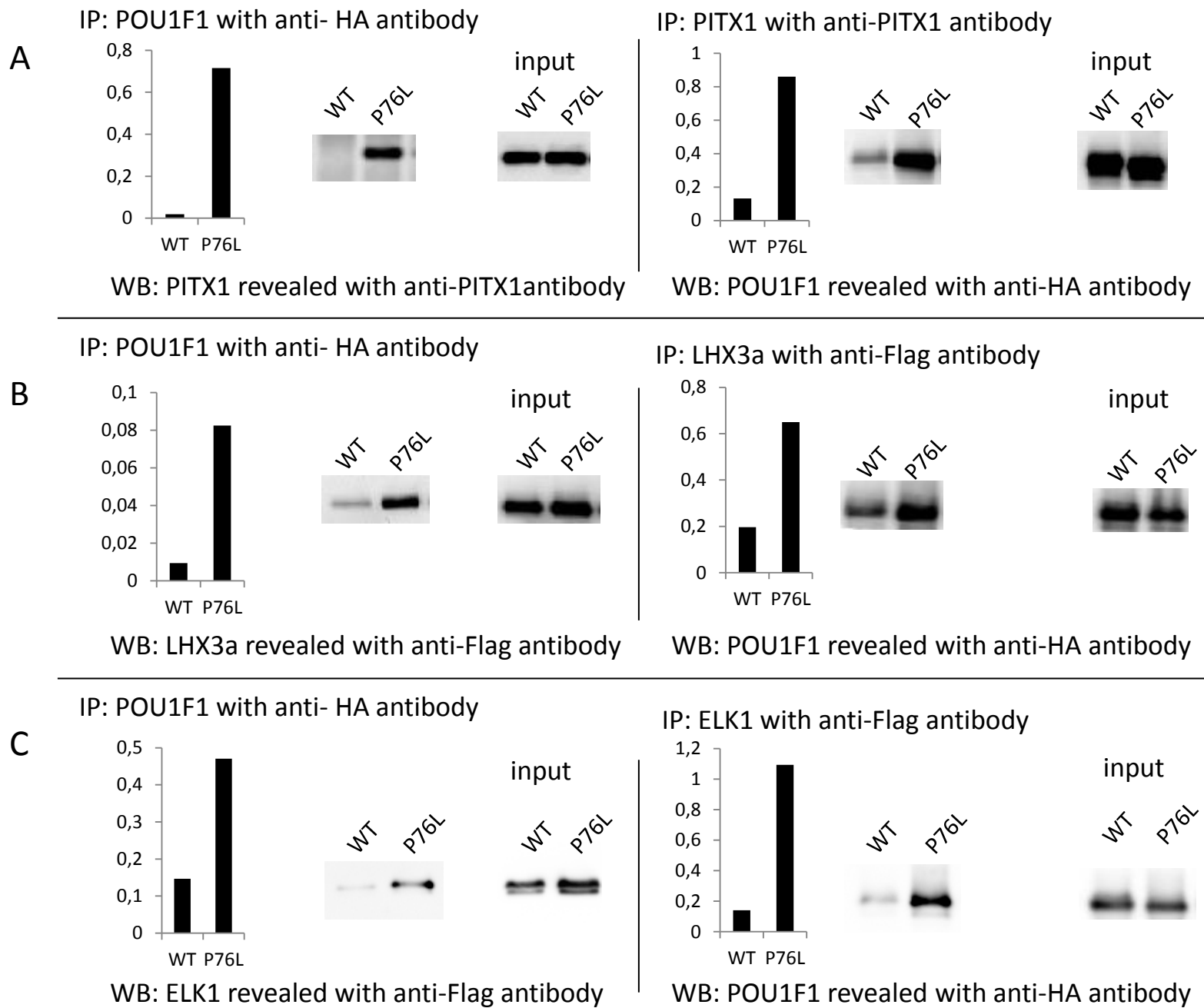


Figure 5



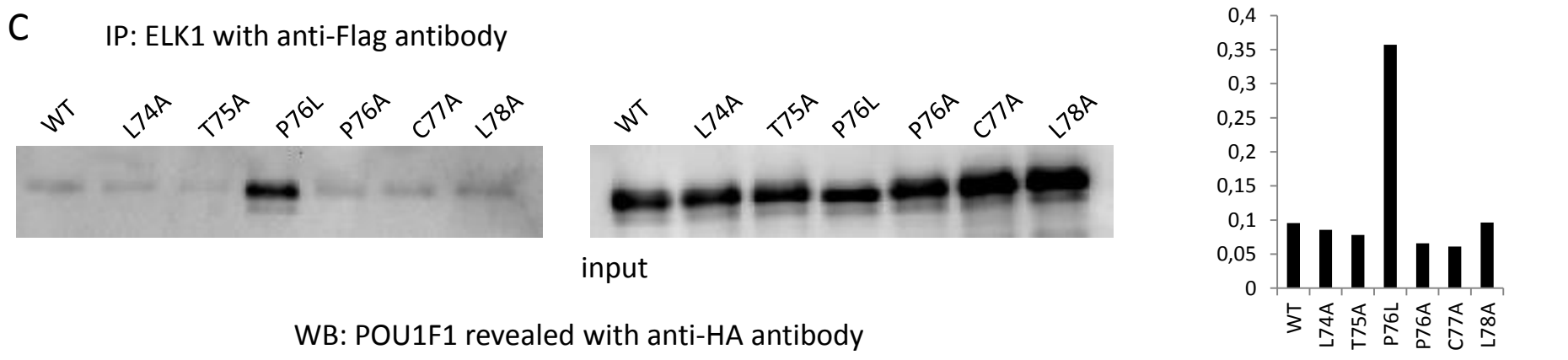
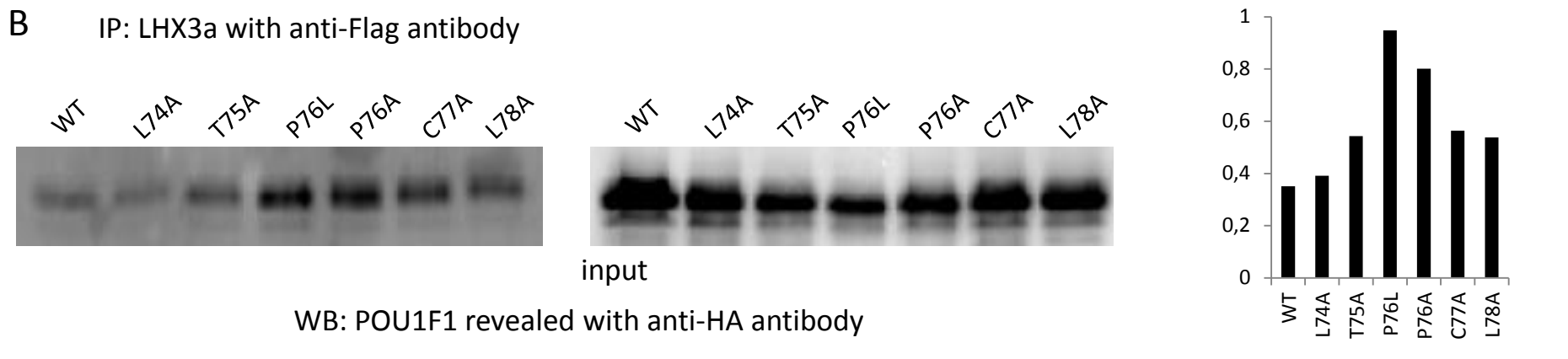
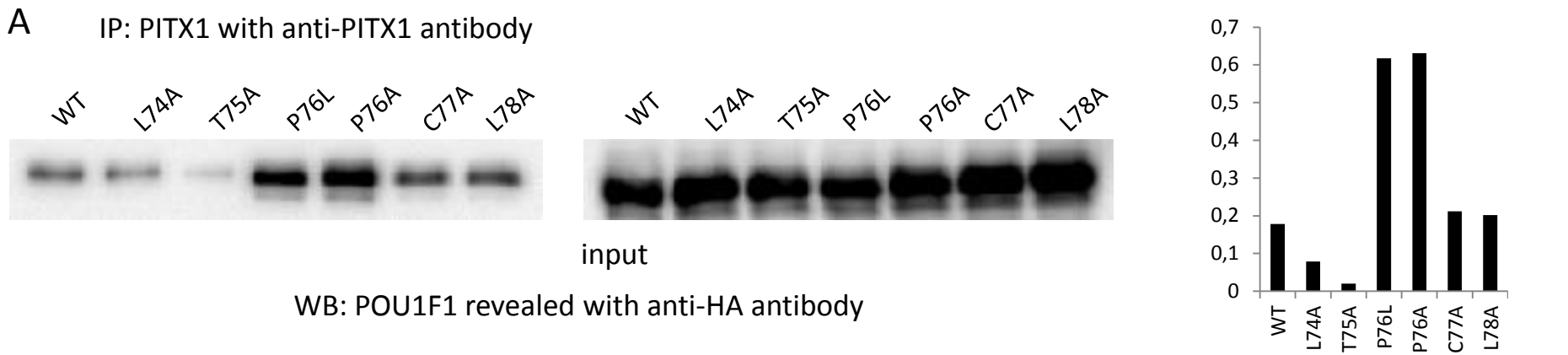


Figure 6

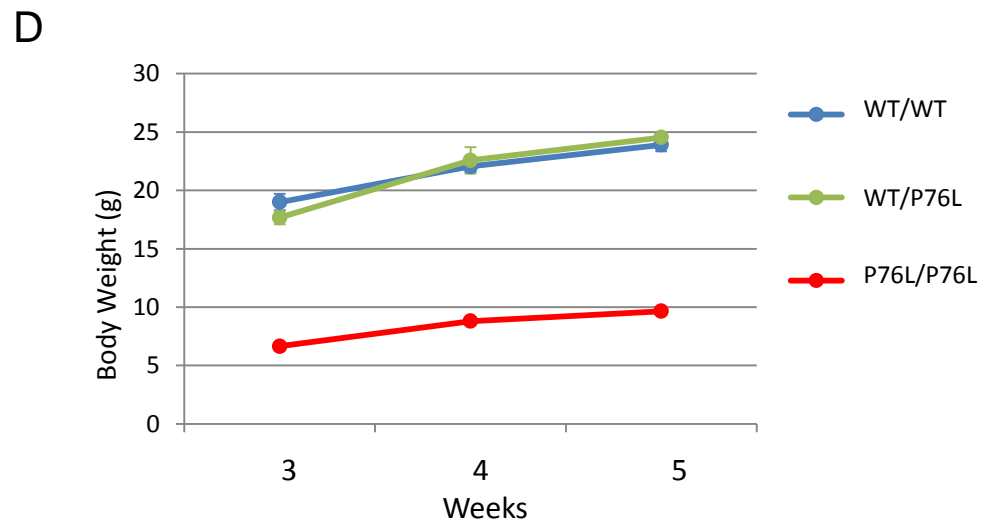
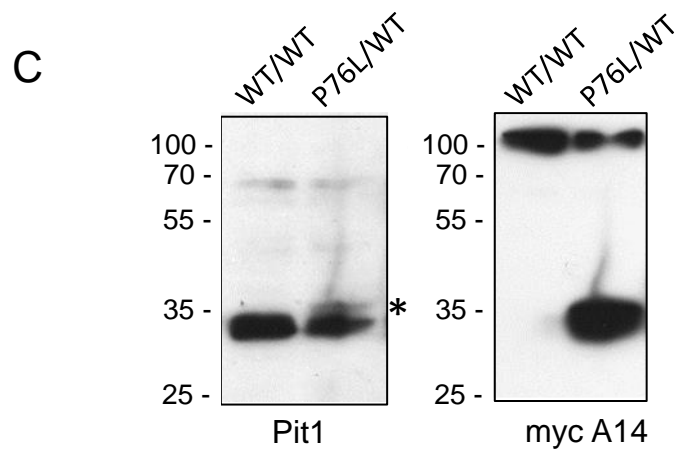
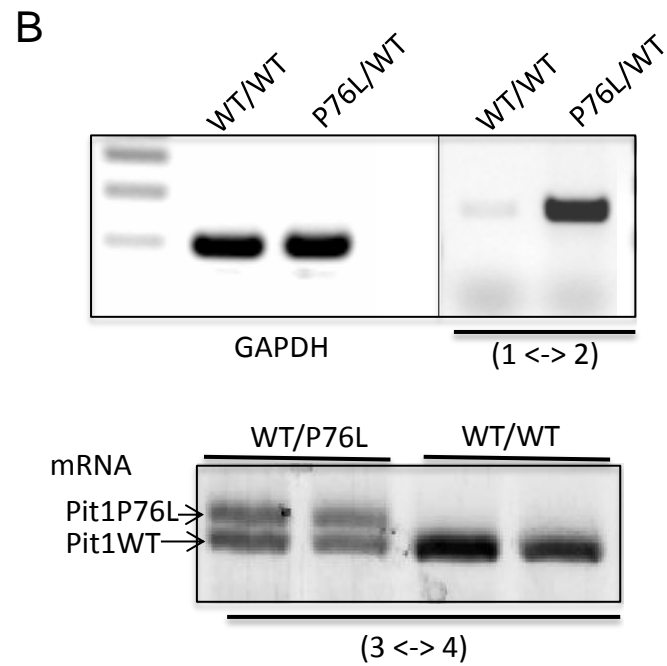
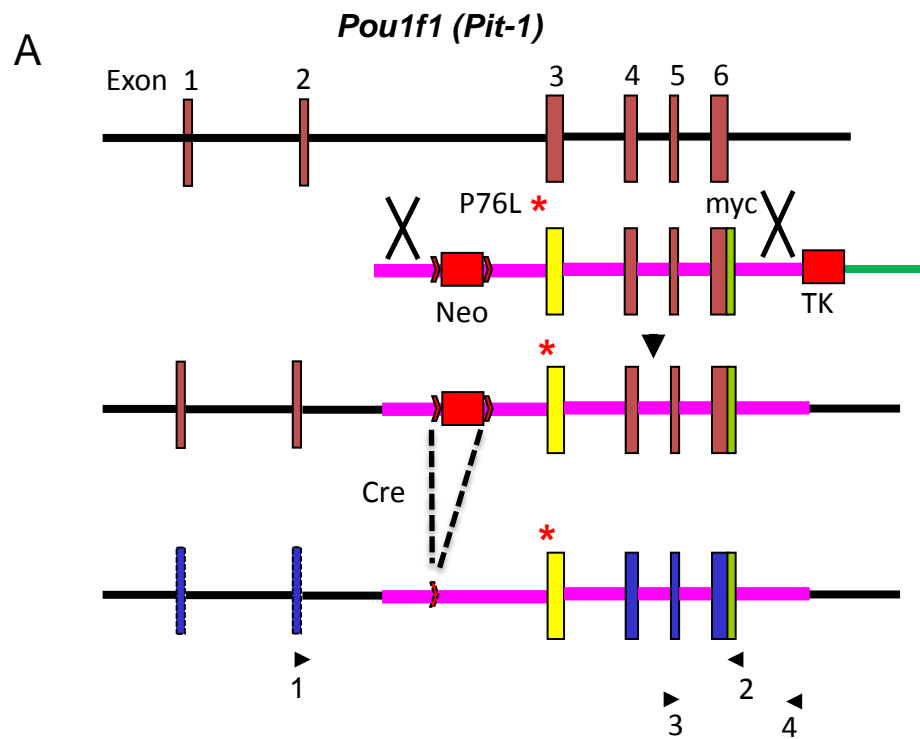


Figure 7